BELLE-CONF-0119

A Search for the Electric Dipole Moment of the τ lepton

The Belle Collaboration

Abstract

We have searched for CP violation in the reaction $e^+e^- \to \tau^+\tau^-$ with the Belle detector at the KEKB collider. Parametrizing CP violation by the electric dipole form-factor $d_\tau(s)$, which we measure using the method of optimized observables, we obtain preliminary upper limits of $|Re(d_\tau)| < 6.7 \times 10^{-17}$ecm and $|Im(d_\tau)| < 2.2 \times 10^{-17}$ecm with a confidence level of 95% from a sample of about 9.4 million τ pairs at $\sqrt{s} = 10.58$ GeV. This represents an improvement in statistical precision by an order of magnitude, compared to previous d_τ measurements; systematic effects are still being studied.

Typeset using REVTEX

K. Abe[9], K. Abe[37], R. Abe[27], I. Adachi[9], Byoung Sup Ahn[15], H. Aihara[39], M. Akatsu[20], K. Asai[21], M. Asai[10], Y. Asano[44], T. Aso[43], V. Aulchenko[2], T. Aushev[13], A. M. Bakich[35], E. Banas[25], S. Behari[9], P. K. Behera[45], D. Beiline[2], A. Bondar[2], A. Bozek[25], T. E. Browder[8], B. C. K. Casey[8], P. Chang[24], Y. Chao[24], K.-F. Chen[24], B. G. Cheon[34], R. Chistov[13], S.-K. Choi[7], Y. Choi[34], L. Y. Dong[12], J. Dragic[18], A. Drutskoy[13], S. Eidelman[2], V. Eiges[13], Y. Enari[20], C. W. Everton[18], F. Fang[8], H. Fujii[9], C. Fukunaga[41], M. Fukushima[11], A. Garmash[2,9], A. Gordon[18], K. Gotow[46], H. Guler[8], R. Guo[22], J. Haba[9], H. Hamasaki[9], K. Hanagaki[31], F. Handa[38], K. Hara[29], T. Hara[29], N. C. Hastings[18], H. Hayashii[21], M. Hazumi[29], E. M. Heenan[18], Y. Higasino[20], I. Higuchi[38], T. Higuchi[39], T. Hirai[40], H. Hirano[42], T. Hojo[29], T. Hokuue[20], Y. Hoshi[37], K. Hoshina[42], S. R. Hou[24], W.-S. Hou[24], S.-C. Hsu[24], H.-C. Huang[24], Y. Igarashi[9], T. Iijima[9], H. Ikeda[9], K. Ikeda[21], K. Inami[20], A. Ishikawa[20], H. Ishino[40], R. Itoh[9], G. Iwai[27], H. Iwasaki[9], Y. Iwasaki[9], D. J. Jackson[29], P. Jalocha[25], H. K. Jang[33], M. Jones[8], R. Kagan[13], H. Kakuno[40], J. Kaneko[40], J. H. Kang[48], J. S. Kang[15], P. Kapusta[25], N. Katayama[9], H. Kawai[3], H. Kawai[39], Y. Kawakami[20], N. Kawamura[1], T. Kawasaki[27], H. Kichimi[9], D. W. Kim[34], Heejong Kim[48], H. J. Kim[48], Hyunwoo Kim[15], S. K. Kim[33], T. H. Kim[48], K. Kinoshita[5], S. Kobayashi[32], S. Koishi[40], H. Konishi[42], K. Korotushenko[31], P. Krokovny[2], R. Kulasiri[5], S. Kumar[30], T. Kuniya[32], E. Kurihara[3], A. Kuzmin[2], Y.-J. Kwon[48], J. S. Lange[6], S. H. Lee[33], C. Leonidopoulos[31], Y.-S. Lin[24], D. Liventsev[13], R.-S. Lu[24], D. Marlow[31], T. Matsubara[39], S. Matsui[20], S. Matsumoto[4], T. Matsumoto[20], Y. Mikami[38], K. Misono[20], K. Miyabayashi[21], H. Miyake[29], H. Miyata[27], L. C. Moffitt[18], G. R. Moloney[18], G. F. Moorhead[18], N. Morgan[46], S. Mori[44], T. Mori[4], A. Murakami[32], T. Nagamine[38], Y. Nagasaka[10], Y. Nagashima[29], T. Nakadaira[39], T. Nakamura[40], E. Nakano[28], M. Nakao[9], H. Nakazawa[4], J. W. Nam[34], Z. Natkaniec[25], K. Neichi[37], S. Nishida[16], O. Nitoh[42], S. Noguchi[21], T. Nozaki[9], S. Ogawa[36], T. Ohshima[20], Y. Ohshima[40], T. Okabe[20], T. Okazaki[21], S. Okuno[14], S. L. Olsen[8], H. Ozaki[9], P. Pakhlov[13], H. Palka[25], C. S. Park[33], C. W. Park[15], H. Park[17], L. S. Peak[35], M. Peters[8], L. E. Piilonen[46], E. Prebys[31], J. L. Rodriguez[8], N. Root[2], M. Rozanska[25], K. Rybicki[25], J. Ryuko[29], H. Sagawa[9], Y. Sakai[9], H. Sakamoto[16], M. Satapathy[45], A. Satpathy[9,5], S. Schrenk[5], S. Semenov[13], K. Senyo[20], Y. Settai[4], M. E. Sevior[18], H. Shibuya[36], B. Shwartz[2], A. Sidorov[2], S. Stanič[44], A. Sugi[20], A. Sugiyama[20], K. Sumisawa[9], T. Sumiyoshi[9], J.-I. Suzuki[9], K. Suzuki[3], S. Suzuki[47], S. Y. Suzuki[9], S. K. Swain[8], H. Tajima[39], T. Takahashi[28], F. Takasaki[9], M. Takita[29], K. Tamai[9], N. Tamura[27], J. Tanaka[39], M. Tanaka[9], Y. Tanaka[19], G. N. Taylor[18], Y. Teramoto[28], M. Tomoto[9], T. Tomura[39], S. N. Tovey[18], K. Trabelsi[8], T. Tsuboyama[9], T. Tsukamoto[9], S. Uehara[9], K. Ueno[24], Y. Unno[3], S. Uno[9], Y. Ushiroda[9], S. E. Vahsen[31], K. E. Varvell[35], C. C. Wang[24], C. H. Wang[23], J. G. Wang[46], M.-Z. Wang[24], Y. Watanabe[40], E. Won[33], B. D. Yabsley[9], Y. Yamada[9], M. Yamaga[38], A. Yamaguchi[38], H. Yamamoto[8], T. Yamanaka[29], Y. Yamashita[26], M. Yamauchi[9], S. Yanaka[40], M. Yokoyama[39], K. Yoshida[20], Y. Yusa[38], H. Yuta[1], C. C. Zhang[12], J. Zhang[44], H. W. Zhao[9], Y. Zheng[8], V. Zhilich[2], and D. Žontar[44]

[1]Aomori University, Aomori
[2]Budker Institute of Nuclear Physics, Novosibirsk
[3]Chiba University, Chiba
[4]Chuo University, Tokyo
[5]University of Cincinnati, Cincinnati OH

[6]University of Frankfurt, Frankfurt
[7]Gyeongsang National University, Chinju
[8]University of Hawaii, Honolulu HI
[9]High Energy Accelerator Research Organization (KEK), Tsukuba
[10]Hiroshima Institute of Technology, Hiroshima
[11]Institute for Cosmic Ray Research, University of Tokyo, Tokyo
[12]Institute of High Energy Physics, Chinese Academy of Sciences, Beijing
[13]Institute for Theoretical and Experimental Physics, Moscow
[14]Kanagawa University, Yokohama
[15]Korea University, Seoul
[16]Kyoto University, Kyoto
[17]Kyungpook National University, Taegu
[18]University of Melbourne, Victoria
[19]Nagasaki Institute of Applied Science, Nagasaki
[20]Nagoya University, Nagoya
[21]Nara Women's University, Nara
[22]National Kaohsiung Normal University, Kaohsiung
[23]National Lien-Ho Institute of Technology, Miao Li
[24]National Taiwan University, Taipei
[25]H. Niewodniczanski Institute of Nuclear Physics, Krakow
[26]Nihon Dental College, Niigata
[27]Niigata University, Niigata
[28]Osaka City University, Osaka
[29]Osaka University, Osaka
[30]Panjab University, Chandigarh
[31]Princeton University, Princeton NJ
[32]Saga University, Saga
[33]Seoul National University, Seoul
[34]Sungkyunkwan University, Suwon
[35]University of Sydney, Sydney NSW
[36]Toho University, Funabashi
[37]Tohoku Gakuin University, Tagajo
[38]Tohoku University, Sendai
[39]University of Tokyo, Tokyo
[40]Tokyo Institute of Technology, Tokyo
[41]Tokyo Metropolitan University, Tokyo
[42]Tokyo University of Agriculture and Technology, Tokyo
[43]Toyama National College of Maritime Technology, Toyama
[44]University of Tsukuba, Tsukuba
[45]Utkal University, Bhubaneswer
[46]Virginia Polytechnic Institute and State University, Blacksburg VA
[47]Yokkaichi University, Yokkaichi
[48]Yonsei University, Seoul

I. INTRODUCTION

CP violation(CPV) has been observed in the quark sector, in the neutral kaon system. B-factory experiments, including the Belle experiment, are currently searching for CPV in B meson mixing and decay, to test the predictions of the CKM model. The standard model does not predict any appreciable CPV in the lepton sector, but such effects can appear, for example, in multi-Higgs, SUSY and lepto-quark models. New bosons and the Higgs couple strongly with heavy particles through quantum loop effects. Therefore the τ lepton could exhibit measurable CP violation because of its large mass.

In the analysis reported here, we searched for CPV at the $\gamma\tau\tau$ vertex by measuring CP-odd triple momentum correlation observables. If CPV exists, the mean value of these observable should be non-zero. CPV at the production vertex can in general be parametrized by an electric dipole form-factor $d_\tau(s)$, described by the CPV effective Lagrangian:

$$\mathcal{L}_{CP} = -\frac{i}{2}\bar{\tau}\sigma^{\mu\nu}\gamma_5\tau d_\tau(s) F_{\mu\nu} \tag{1}$$

where $F_{\mu\nu}$ is the electromagnetic field tensor. (Hereafter, we will write $d_\tau(s) = d_\tau$, and use the abbreviation "EDM" (electric dipole moment) for this quantity.)

Previously, LEP and the ARGUS experiment have reported upper limits on d_τ of $|d_\tau| < 3.1 \times 10^{-16} e\text{cm}$ [1] and $|Re(d_\tau)/Im(d_\tau)| < 4.6/1.8 \times 10^{-16} e\text{cm}$ [2] respectively.

II. OBSERVABLES

In the process $e^+(\boldsymbol{p})e^-(-\boldsymbol{p}) \to \tau^+(\boldsymbol{k}, \boldsymbol{S}_+)\tau^-(-\boldsymbol{k}, \boldsymbol{S}_-)$ the spin density matrix with EDM d_τ is given by [3]

$$\mathcal{M}_{\rm prod} = \mathcal{M}_{\rm SM} + Re(d_\tau)\mathcal{M}_{Re} + Im(d_\tau)\mathcal{M}_{Im} + |d_\tau|^2\mathcal{M}_{d^2} \tag{2}$$

$$\begin{aligned}\mathcal{M}_{\rm SM} \propto\; & k_0^2 + m_\tau^2 + |\boldsymbol{k}^2|(\hat{\boldsymbol{k}}\hat{\boldsymbol{p}})^2 - \boldsymbol{S}_+\boldsymbol{S}_-|\boldsymbol{k}|^2(1-(\hat{\boldsymbol{k}}\hat{\boldsymbol{p}})^2) \\ & +2(\hat{\boldsymbol{k}}\boldsymbol{S}_+)(\hat{\boldsymbol{k}}\boldsymbol{S}_-)(|\boldsymbol{k}|^2 + (k_0 - m_\tau)^2(\hat{\boldsymbol{k}}\hat{\boldsymbol{p}})^2) + 2k_0^2(\hat{\boldsymbol{p}}\boldsymbol{S}_+)(\hat{\boldsymbol{p}}\boldsymbol{S}_-) \\ & -2k_0(k_0 - m_\tau)\hat{\boldsymbol{k}}\hat{\boldsymbol{p}}((\hat{\boldsymbol{k}}\boldsymbol{S}_+)(\hat{\boldsymbol{p}}\boldsymbol{S}_-) + (\hat{\boldsymbol{k}}\boldsymbol{S}_-)(\hat{\boldsymbol{p}}\boldsymbol{S}_+))\end{aligned} \tag{3}$$

$$\begin{aligned}\mathcal{M}_{Re} \propto 2k_0|\boldsymbol{k}|[\; & -(m_\tau + (k_0 - m_\tau)(\hat{\boldsymbol{k}}\hat{\boldsymbol{p}})^2)(\boldsymbol{S}_+ \times \boldsymbol{S}_-)\hat{\boldsymbol{k}} \\ & + k_0(\hat{\boldsymbol{k}}\hat{\boldsymbol{p}})(\boldsymbol{S}_+ \times \boldsymbol{S}_-)\hat{\boldsymbol{p}} \quad]\end{aligned} \tag{4}$$

$$\begin{aligned}\mathcal{M}_{Im} \propto 2k_0|\boldsymbol{k}|[\; & -(m_\tau + (k_0 - m_\tau)(\hat{\boldsymbol{k}}\hat{\boldsymbol{p}})^2)(\boldsymbol{S}_+ - \boldsymbol{S}_-)\hat{\boldsymbol{k}} \\ & + k_0(\hat{\boldsymbol{k}}\hat{\boldsymbol{p}})(\boldsymbol{S}_+ - \boldsymbol{S}_-)\hat{\boldsymbol{p}} \quad]\end{aligned} \tag{5}$$

$$\mathcal{M}_{d^2} \propto k_0^2|\boldsymbol{k}|^2 \cdot \quad 4(1-(\hat{\boldsymbol{k}}\hat{\boldsymbol{p}})^2)(1-\boldsymbol{S}_+\boldsymbol{S}_-) \tag{6}$$

where hats denote unit momenta, k_0 is the energy of the $\tau^\pm$, m_τ is the τ mass, $\boldsymbol{p}$ is the three momentum of the e^+, $\boldsymbol{k}$ is the three momentum of the τ^+, and $\boldsymbol{S}_\pm$ are the spin vectors for $\tau^\pm$. In writing these equations we have assumed unpolarized e^+ and e^- beams and neglected the electron mass.

The total differential cross section of the process $e^+e^- \to \tau^+\tau^- \to X^+Y^-$ can be factorized into matrix elements for the τ-pair production vertex, $\mathcal{M}_{\rm prod}$, and the τ-decay vertex, $\mathcal{M}_{\rm dec}$, as

$$d\sigma_{\rm tot} \sim \mathcal{M}_{\rm prod} \cdot \mathcal{M}_{\rm dec}. \tag{7}$$

$\mathcal{M}_{\rm dec}$ is assumed not to have any EDM contribution.

In the analysis, we form so-called optimized observables [3]

$$\mathcal{O}_{Re} = \frac{\mathcal{M}_{Re}}{\mathcal{M}_{\rm SM}}, \quad \mathcal{O}_{Im} = \frac{\mathcal{M}_{Im}}{\mathcal{M}_{\rm SM}}, \tag{8}$$

using the factorization method for the total cross section; these observables maximize the sensitivity to the EDM. In the case of a small EDM value, since we can ignore the d_τ^2 term, the mean values of these observables show a linear dependence on the real and imaginary parts of the EDM,

$$\langle \mathcal{O}_{Re} \rangle = C_{Re} Re(d_\tau), \quad \langle \mathcal{O}_{Im} \rangle = C_{Im} Im(d_\tau). \tag{9}$$

Experimentally, we cannot know the τ flight direction and the τ spin orientation from the observed particles. Therefore, for each event we find the range of kinematic configurations which are consistent with the observed final state, and use the average value of the amplitudes. In the case that both τ leptons decay to hadrons ($\tau \to \pi\nu$ or $\rho\nu$), the τ flight direction is calculated with twofold ambiguity and we take an average of the two solutions. In the case that one or both τ decay leptonically ($\tau \to e\nu\bar{\nu}$ or $\mu\nu\bar{\nu}$), we use a Monte Carlo method. For each semi-leptonic decay, there is an additional ambiguity due to the effective mass of the $\nu\bar{\nu}$ pair. For each event, we make 100 tries using a hit and miss approach for the effective mass(es), and take an average over the amplitudes of successful tries in which a consistent τ direction can be reconstructed.

III. DATA AND MONTE CARLO SAMPLES

In this analysis, we use 9.4 million τ pairs (10.3 fb^{-1}), accumulated with the Belle detector [4] at the KEKB accelerator [5]. KEKB is an asymmetric e^+e^- collider with a beam crossing angle of 22 mrad. Its center of mass energy is 10.58 GeV, corresponding to the $\Upsilon(4S)$ resonance, with beam energies of 8 and 3.5 GeV for the electrons and positrons respectively.

Belle is a general purpose detector with an asymmetric structure along the beam direction. Among the detector elements, the Central Drift Chamber(CDC) and the Silicon Vertex Detector(SVD) are essential to obtain the momentum vectors of charged particles. The combined information from the Silica Aerogel Cherenkov Counter(ACC), the Time-Of-Flight counter(TOF), the CsI Electromagnetic Calorimeter(ECL) and the $\mu/\mathrm{K_L}$ detector(KLM) are used for the electron and muon identification.

Monte Carlo(MC) event generators, KORALB/TAUOLA [6], are used for the τ-pair production and decays. Detector simulation is performed by a GEANT based program GSIM. Actual data and MC generated events are reconstructed by the same program written by the Belle collaboration. We used a sample of 110 million MC events, which corresponds to a luminosity of 121 fb^{-1}. In order to investigate the effects of background from non τ-pair events, we generate MC samples for the continuum ($e^+e^- \to q\bar{q}$) and for $B\bar{B}$ ($e^+e^- \to \Upsilon(4S) \to B\bar{B}$) production using the QQ [7] program, and two-photon processes ($2\gamma \to l^+l^-, q\bar{q}$) using the AAFHB [8] program.

IV. EVENT SELECTION

We choose the eight final state τ-pair modes: $e\mu, e\pi, \mu\pi, e\rho, \mu\rho, \pi\rho, \pi\pi$ and $\rho\rho$. All the final states particles are reconstructed.

Each charged track is required to have a transverse momentum of $p_t > 0.1$ GeV/c. Photon candidates should deposit an energy of $E > 0.1$ GeV in the ECL. Signal events are required to have two charged tracks with zero net-charge and no photon except from the daughter of $\rho^{\pm}$.

An electron track is identified if it satisfies the following conditions:(1) E/p is greater than 0.8 where E is the ECL cluster energy associated with the track of the momentum p and (2) the electron probability determined from both shower shape in the ECL and dE/dx in the CDC is greater than 0.6. The efficiency is better than 90% and the fake rate is smaller than 1%. A muon track is identified by its range passing through KLM detector. We require the probability to be greater than 0.95. Muon detection efficiency is about 90% and its fake rate is about 2%. A pion track is identified by the combination of the probabilities: (1) the hadron probability by KLM is greater then 0.95, (2) the electron probability in terms of E/p ratio is less than 0.4, (3) the combined electron probability by means of both shower shape and dE/dx is less than 0.1, (4) a likelihood ratio of pion to kaon is greater than 0.6, where the ratio is defined as $L(\pi)/(L(\pi)+L(K))$. The efficiency is 66%, while the fake rate is about 5%. For pion selection, a tight cut is applied to reduce the fake rate.

A $\rho^{\pm}$ is reconstructed from a charged track and π^0, where the track is required not to be an electron, muon or kaon, and the π^0 (reconstructed from a $\gamma\gamma$ pair) should have an invariant mass between 110 and 150 MeV and momentum of $p > 0.2$ GeV/c. FIG. 1 shows the $\pi^{\pm}\pi^0$ invariant mass distribution for the selected $\rho^{\pm}$.

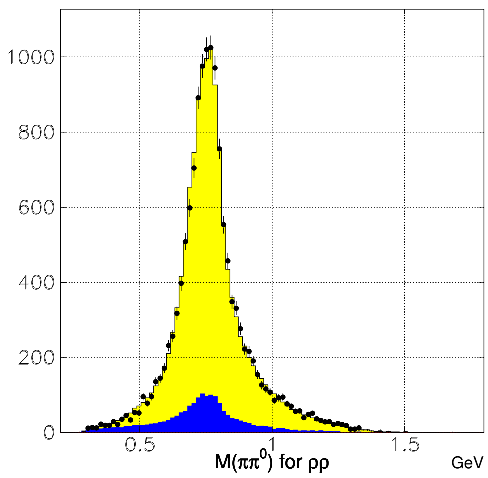

FIG. 1. $\pi^{\pm}\pi^0$ invariant mass distribution. The points with error bars are the data and the histogram is the MC expectation. The latter is scaled by the total number of entries. The solid blue histogram is the background component in the MC.

In order to reduce the background and enhance the particle-identification power, the leptonic particle e/μ is required to be within the barrel region, $-0.60 < \cos\theta_{\mathrm{lab.}} < 0.83$, while the $\pi^{\pm}$ is required to be within $-0.50 < \cos\theta_{\mathrm{lab.}} < 0.62$. Furthermore, their electron momentum should be greater than 0.5 GeV/c, the muon and pion momenta should be greater than 1.2 GeV/c and the $\rho^{\pm}$ momentum should be greater than 1.0 GeV/c. All these momenta are calculated in the laboratory frame.

In order to suppress the 2 photon background we require the missing momentum not to be directed along the beam pipe ($-0.950 < \cos\theta_{\mathrm{missing,lab.}} < 0.985$). To reject Bhabha and $\mu\mu$ backgrounds, we require that the sum of the charged track momenta in the CM frame be less than 9 GeV/c. For the $e\pi$ mode, we remove events in which the opening angle of the two charged particles in the r-ϕ plane is greater than 175 degrees and the sum of the charged track momenta in the CM frame is greater than 6 GeV. The hardware trigger conditions are also included in the MC simulation.

Finally, we reject events in which the τ flight direction cannot be reconstructed kinematically. These events include background from non-τ processes and τ pairs with hard initial state radiation.

V. SELECTED SAMPLES

The yields of the 8 selected modes are given in TABLE I. We have selected a total of 347,000 events. The dominant background sources for each mode are also listed with their contamination rates, which are predicted from the MC data samples as described above. A number of hadronic τ decays with two or more π^0s make a large contribution to the background. For the modes including $\pi^{\pm}$, there are additional backgrounds due to fake pions from mis-identified muons. The background from 2 photon processes is estimated to be a few %. Backgrounds from Bhabhas, $\mu\mu$ and multi-hadronic processes are found from MC to be less than 1%.

The distributions of $\cos\theta$ in the laboratory frame are shown in FIG. 2.

TABLE I. Yield, purity and background fractions in the selected samples. The purity is determined from MC. The error is from MC statistics.

mode	yield	purity	background mode (contamination rate%)
$e\mu$	80535	$96.4 \pm 0.5\%$	$2\gamma \to \mu\mu(1.9\%)$, $\tau\tau \to e\pi(1.3\%)$
$e\pi$	32985	$86.7 \pm 0.7\%$	$\tau\tau \to e\rho(6.4\%)$ $e\mu(3.0\%)$
$\mu\pi$	31111	$84.9 \pm 0.7\%$	$\tau\tau \to \mu\rho(6.2\%)$ $\mu\mu(2.8\%)$, $2\gamma \to \mu\mu(2.0\%)$
$e\rho$	83750	$93.4 \pm 0.4\%$	$\tau\tau \to e\pi\pi^0\pi^0(4.9\%)$
$\mu\rho$	73750	$92.6 \pm 0.4\%$	$\tau\tau \to \mu\pi\pi^0\pi^0(4.5\%)$ $\pi\rho(1.0\%)$
$\pi\rho$	32467	$82.5 \pm 0.6\%$	$\tau\tau \to \rho\rho(6.0\%)$ $\pi\pi\pi^0\pi^0(4.3\%)$ $\mu\rho(2.6\%)$
$\pi\pi$	5571	$77.2 \pm 1.5\%$	$\tau\tau \to \pi\rho(10.8\%)$ $\pi\mu(5.2\%)$
$\rho\rho$	6885	$87.8 \pm 1.3\%$	$\tau\tau \to \rho\pi\pi^0\pi^0(8.8\%)$

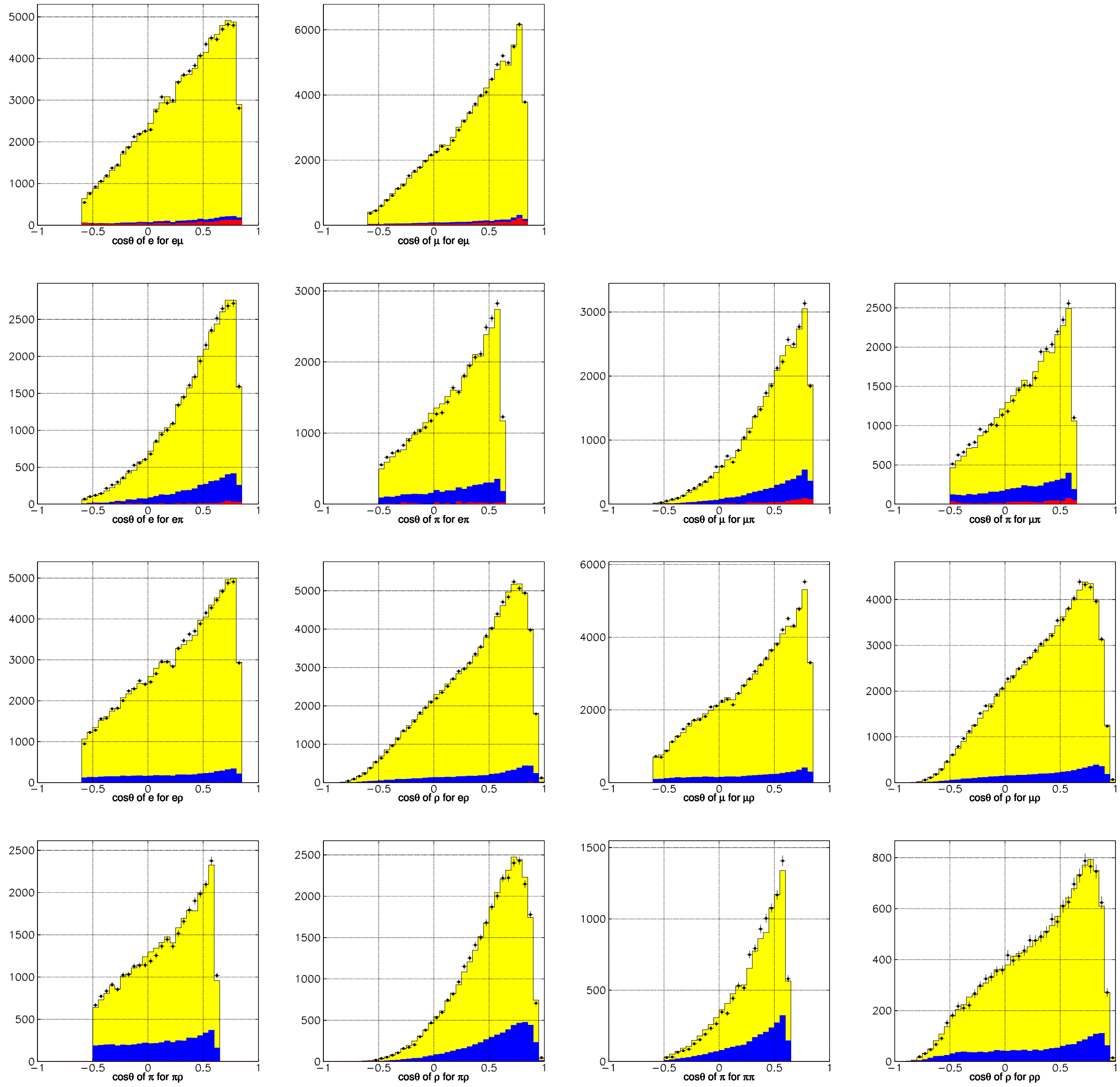

FIG. 2. The $\cos\theta_{\rm lab.}$ distributions. The dots are the experimental data, and the histogram is the MC expectation, which is scaled by the number of entries. The blue(darker) histogram is the background component. The red(middle darker) histogram is the background from non-τ processes.

VI. ANALYSIS

A. Correlation

In order to extract the EDM from the observables, we need to know the conversion coefficients $C_{Re/Im}$ defined in eq.(9). If all the kinematical quantities needed to calculate the amplitudes were known, the conversion coefficients could be obtained from an analytical calculation. However, there are ambiguities in these quantities and smearing from the detector resolution. These effects change the sensitivity to $C_{Re/Im}$. Since the detector acceptance is asymmetric along the beam direction and there is an azimuthal rotation due to the beam crossing angle, the relation between the optimal observables and the EDM may have some offset.

Therefore, the relation between the EDM and the observables should be changed:

$$\langle \mathcal{O}_{Re} \rangle^{eff} = a_{Re}^{eff} \cdot Re(d_\tau) + b_{Re}^{eff}, \quad \langle \mathcal{O}_{Im} \rangle^{eff} = a_{Im}^{eff} \cdot Im(d_\tau) + b_{Im}^{eff}. \tag{10}$$

FIG. 3 shows the behavior of the observables as a function of the EDM parameters $Re(d_\tau)$ and $Im(d_\tau)$ for the $\pi\rho$ mode. The observable distributions are obtained by weighting the MC events with the full spin density matrix elements. By fitting eq.(10) to the distributions, coefficients, $a_{Re/Im}^{eff}$, and offsets, $b_{Re/Im}^{eff}$, are obtained as shown in FIG. 4.

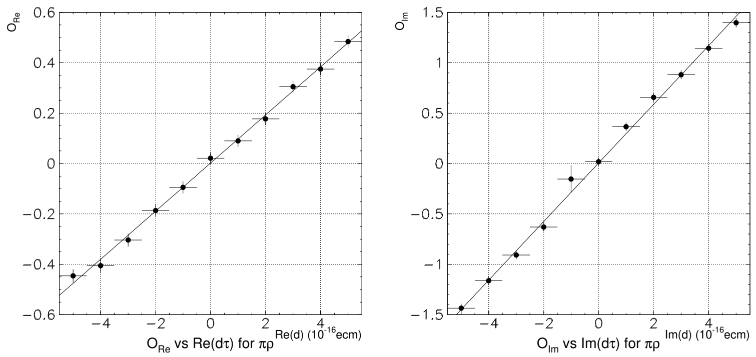

FIG. 3. The relation between the EDM (left:$Re(d_\tau)$, right:$Im(d_\tau)$) and the optimal observable of the $\pi\rho$ final state, obtained from MC. The line shows the result of a linear fit.

The coefficients $a_{Re/Im}^{eff}$ give the sensitivity of $\langle \mathcal{O}_{Re} \rangle (\langle \mathcal{O}_{Im} \rangle)$ to $Re(d_\tau)(Im(d_\tau))$. We see a high sensitivity to $Re(d_\tau)$ in the $\pi\rho$ and $\rho\rho$ modes, and to $Im(d_\tau)$ in the $\pi\rho$, $\pi\pi$ and $\rho\rho$ modes. The lower sensitivity to $Re(d_\tau)$ in the $\pi\pi$ mode is due to the behavior of $\mathcal{M}_{Im}$ and the ambiguity of the τ flight direction. We also see a low sensitivity for the other modes, which include leptons, because of the lack of information about the $\tau^+\tau^-$ and their spin directions due to the extra missing neutrino(s).

B. Measurement of observables

The distributions of the measured $\mathcal{O}_{Re}$ and $\mathcal{O}_{Im}$ are shown in FIG. 5 and compared with a MC simulation with zero EDM. Small differences between the data and MC are seen in

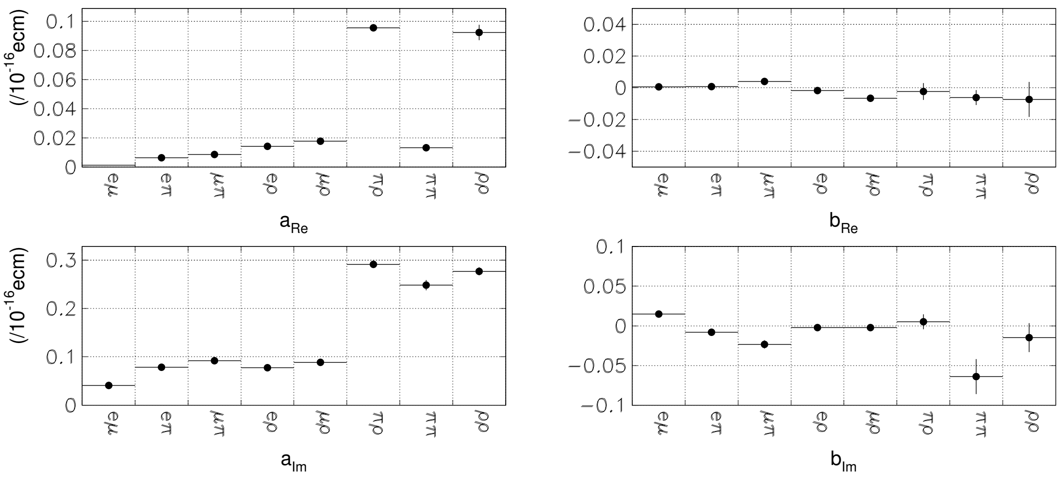

FIG. 4. The sensitivity $a^{eff}_{Re/Im}$(left) and offset $b^{eff}_{Re/Im}$(right) for each mode from MC. The top figures show the parameters for the $Re(d_\tau)$ and the bottom ones show the parameters for the $Im(d_\tau)$. The errors are due to the MC statistics.

some modes. These are discussed below in detail. The mean values of $\mathcal{O}_{Re}$ and $\mathcal{O}_{Im}$ are summarized in TABLE II for each mode.

The values of $Re(d_\tau)$ and $Im(d_\tau)$ can be extracted using the coefficients $a^{eff}_{Re/Im}$ and $b^{eff}_{Re/Im}$, as described in the previous section. The results for $Re(d_\tau)$ and $Im(d_\tau)$ are listed in TABLE III.

C. Systematic errors

In this analysis we rely on the MC simulation in the evaluation of the systematic errors. The differences seen in FIG. 2 and FIG. 5 are mainly due to a mismatch of MC to data but may also be due to a non zero EDM value. Here we discuss major sources of systematics which we have investigated so far, while our investigation is still in progress.

(a) The systematic error most affected is the difference of the efficiencies between the data and MC. The $\cos\theta$ and momentum distributions (FIG. 2) in data agree well with MC. However, in the $\cos\theta$ distribution for the $\pi\pi$ mode, there are some differences. We reweighted the MC shape by the ratio of data to MC, and found the systematic uncertainty to be about 40% of the statistical errors of $\mathcal{O}_{Re}$ and $\mathcal{O}_{Im}$.

(b) Another significant error is due to the charge asymmetry of the efficiency. We compared the ratio of the yields $N(A^+B^-)/N(A^-B^+)$ in data and MC, and found the difference to be 2% or less. We vary the efficiencies by $\pm 2\%$ and found the systematic error on the offset of the imaginary part to be at almost the same level as the statistical error of $\mathcal{O}_{Im}$.

(c) In order to check a possible asymmetry from the tracking systems, we analyzed $e^+e^- \to \mu^+\mu^-$ events. We measured the difference between the tracks' polar angles, $\Delta\theta = \theta^+_{\rm CM} - \theta^-_{\rm CM}$, and their azimuthal angles, $\Delta\phi = \phi^+_{\rm CM} - \phi^-_{\rm CM}$, and found small shifts from a back-to-back topology, of magnitude $\Delta\theta = 1.34$ mrad and $\Delta\phi = 0.12$ mrad. By applying an artificial angle shift to one of the charged tracks, we calculated the residual values of the observables

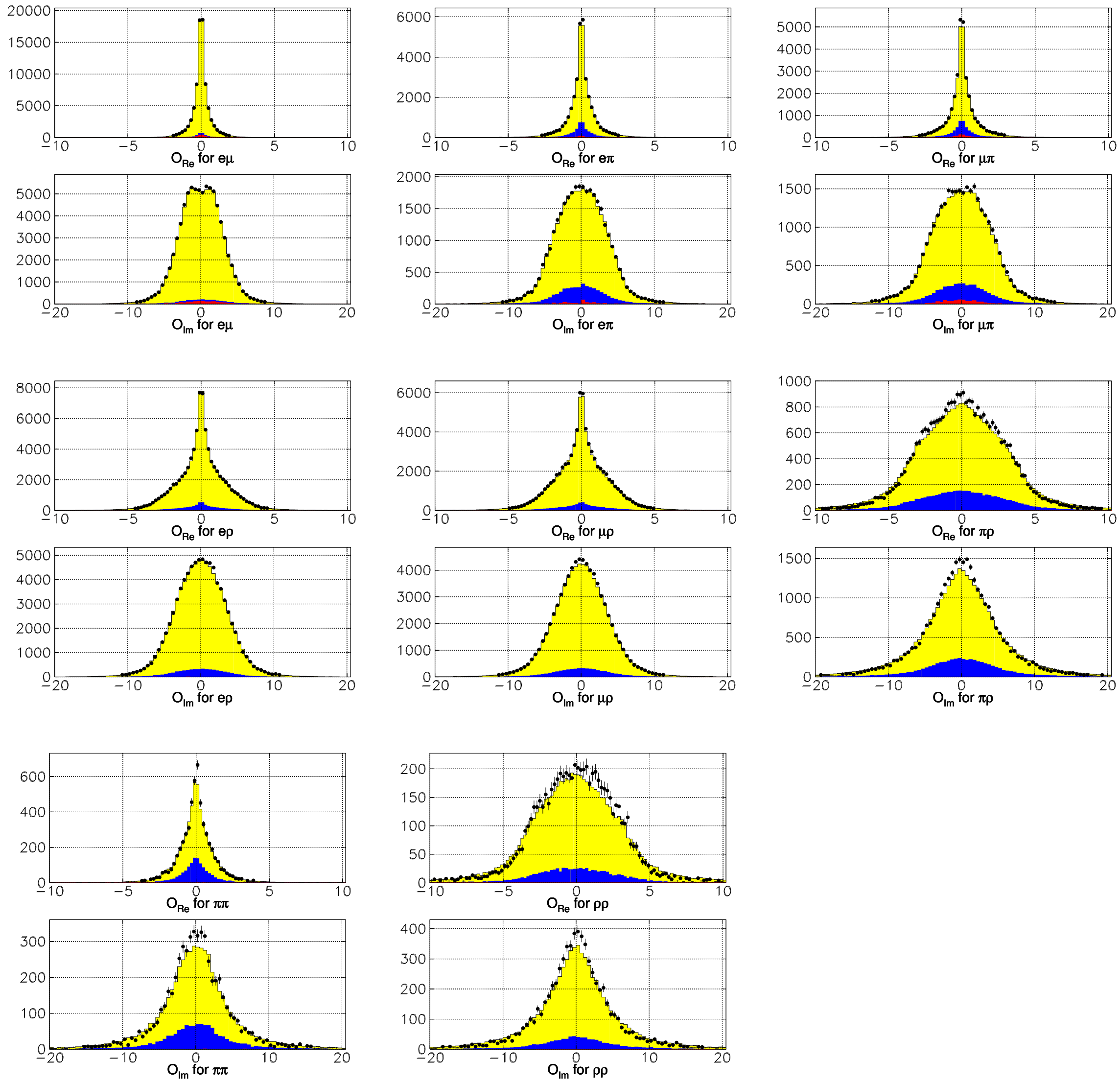

FIG. 5. The distributions of observables, $\mathcal{O}_{Re}$(top) and $\mathcal{O}_{Im}$(bottom), for each mode. The dots are the experimental data and the histogram is the MC expectation scaled by the total number of entries. The blue(darker) and red(middle darker) histograms show the background from τ decays and non-τ processes respectively.

and found the results to be less than 10% of the statistical errors in $\mathcal{O}_{Re}$ and $\mathcal{O}_{Im}$.
(d) As mentioned in section VI B, the width of the observable distribution shown in FIG. 5 is different between data and MC. This difference is mostly due to the difference in resolution on the flight direction. The width of the observable distribution reflects the sensitivity. Therefore, we include its effect in the systematic error on the sensitivity $a_{Re/Im}$. The resulting $\Delta a/a$ is as large as 25%. The difference is largest for the modes with $\rho^{\pm}$ mesons.

Those numbers are taken into account when determining the systematic errors shown in TABLE II and TABLE III.

VII. RESULTS

The mean values of the observables are listed in TABLE II with their systematic errors. The EDMs extracted by eq.(10) are listed in TABLE III and plotted in FIG. 6. The statistical errors of parameters $a_{Re/Im}$ and $b_{Re/Im}$ are included in the statistical errors of the observables.

TABLE II. The mean value of the observable for each final state. The first error is statistical and the second error is the systematic error except for the error of $\Delta a/a$. See the text for a discussion of the systematic error.

mode	$\mathcal{O}_{Re}$	$\mathcal{O}_{Im}$
$e\mu$	$0.0057 \pm 0.0022 \pm 0.0012$	$0.015 \pm 0.010 \pm 0.013$
$e\pi$	$-0.0009 \pm 0.0060 \pm 0.0009$	$-0.029 \pm 0.021 \pm 0.049$
$\mu\pi$	$0.0050 \pm 0.0071 \pm 0.0037$	$0.033 \pm 0.025 \pm 0.058$
$e\rho$	$0.0013 \pm 0.0061 \pm 0.0016$	$0.004 \pm 0.013 \pm 0.008$
$\mu\rho$	$0.0153 \pm 0.0070 \pm 0.0020$	$-0.027 \pm 0.014 \pm 0.014$
$\pi\rho$	$0.0280 \pm 0.0199 \pm 0.0102$	$-0.017 \pm 0.037 \pm 0.062$
$\pi\pi$	$-0.0150 \pm 0.0211 \pm 0.0076$	$0.054 \pm 0.080 \pm 0.074$
$\rho\rho$	$-0.0181 \pm 0.0387 \pm 0.0156$	$-0.052 \pm 0.068 \pm 0.021$

TABLE III. The electric dipole moment, evaluated for each final state. The first error is statistical and second error is the systematic error. See the text for a discussion of the systematic error.

mode	$Re(d_\tau)(10^{-16}e\mathrm{cm})$	$Im(d_\tau)(10^{-16}e\mathrm{cm})$
$e\mu$	$3.86 \pm 1.81 \pm 0.88$	$0.02 \pm 0.26 \pm 0.32$
$e\pi$	$-0.24 \pm 0.95 \pm 0.14$	$-0.27 \pm 0.28 \pm 0.63$
$\mu\pi$	$0.13 \pm 0.83 \pm 0.42$	$0.61 \pm 0.28 \pm 0.64$
$e\rho$	$0.21 \pm 0.44 \pm 0.11$	$0.08 \pm 0.17 \pm 0.10$
$\mu\rho$	$1.23 \pm 0.40 \pm 0.14$	$-0.28 \pm 0.16 \pm 0.16$
$\pi\rho$	$0.32 \pm 0.22 \pm 0.12$	$-0.08 \pm 0.13 \pm 0.21$
$\pi\pi$	$-0.66 \pm 1.64 \pm 0.57$	$0.48 \pm 0.33 \pm 0.30$
$\rho\rho$	$-0.12 \pm 0.44 \pm 0.17$	$-0.13 \pm 0.26 \pm 0.08$

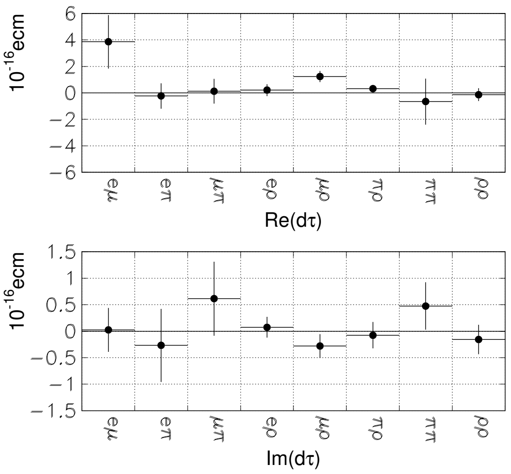

FIG. 6. $Re(d_\tau)$(top) and $Im(d_\tau)$(bottom) for each mode. Errors include the statistical and the systematic ones.

By taking weighted means of the 8 different $\tau^+\tau^-$ modes, we obtain preliminary results for the real and imaginary parts of the τ EDM,

$$Re(d_\tau) = (3.8 \pm 1.7) \times 10^{-17} e\text{cm}, \tag{11}$$
$$Im(d_\tau) = (-0.4 \pm 1.1) \times 10^{-17} e\text{cm}, \tag{12}$$

at $\sqrt{s} = 10.58$ GeV. This represents an improvement in statistical precision by an order of magnitude as compared to previous EDM measurements [1] [2]. However the systematic effects are still being studied.

We can illustrate the sensitivity of the analysis by forming upper limits using the preliminary results and error estimates:

$$|Re(d_\tau)| < 6.7 \times 10^{-17} e\text{cm}, \tag{13}$$
$$|Im(d_\tau)| < 2.2 \times 10^{-17} e\text{cm}, \tag{14}$$

at the 95% confidence level; these are an order of magnitude more restrictive than previous limits.

Acknowledgements

We wish to thank the KEKB accelerator group for the excellent operation of the KEKB accelerator. We acknowledge support from the Ministry of Education, Culture, Sports, Science, and Technology of Japan and the Japan Society for the Promotion of Science; the Australian Research Council and the Australian Department of Industry, Science and Resources; the Department of Science and Technology of India; the BK21 program of the Ministry of Education of Korea and the Center for High Energy Physics sponsored by the KOSEF; the Polish State Committee for Scientific Research under contract No.2P03B 17017; the Ministry of Science and Technology of Russian Federation; the National Science Council and the Ministry of Education of Taiwan; the Japan-Taiwan Cooperative Program of the Interchange Association; and the U.S. Department of Energy.

REFERENCES

[1] L3 Collaboration, M Acciarri et al., Phys. Lett. **B434** (1998) 169; OPAL Collaboration, K Ackerstaff et al., Phys. Lett. **B431** (1998) 188.

[2] H.Albrecht et al. (ARGUS Collaboration), Phys. Lett. **B485** (2000) 37.

[3] W.Bernreuther, O. Nachtmann, P.Overmann, Phys. Rev. **D48** (1993) 78.

[4] K.Abe et al. (Belle Collaboration), 'The Belle Detector', KEK report 2000-4.

[5] KEKB accelerator group, KEKB B Factory Design Report, KEK Report 95-7, 1995; K. Akai et al., Proc. 1999 Particle Accelerator Conference, New York(1999); Y. Funakoshi et al., Proc. 2000 European Particle Accelerator Conference, Vienna(2000).

[6] KORALB(v.2.4): S.Jadach and Z.Was, Comp. Phys. Commun. **85** (1995) 453 and *ibid*, **64** (1991) 267, *ibid*, **36** (1985) 191.

[7] 'QQ - The CLEO Event Generator' (http://www.lns.cornell.edu/public/CLEO/soft/QQ/).

[8] F.A.Berends, P.H.Daverveldt, R.Kleiss, Comp. Phys. Commun. **40** (1986) 285.